Journal of Fundamental and Applied Sciences

ISSN 1112-9867

Available online at http://www.jfas.info

Research Article

Special Issue

AERODYNAMIC SOUND FROM A SAWTOOTH PLATE WITH DIFFERENT THICKNESS

S. R. L. Samion[1], M. S. M. Ali[1] and C. Doolan[2,*]

[1]Malaysia-Japan International Insitute of Technology, University of Technology Malaysia, 54 100 Kuala Lumpur, MALAYSIA

[2]School of Mechanical and Manufacturing Engineering, University of New South Wales, NSW 2052, AUSTRALIA

Published online: 24 November 2017

ABSTRACT

Acoustic performance of an airfoil can be improved with the serrated leading or trailing edge. A sawtooth plate is one of the serration shapes. In this study, the effect of sawtooth plate thickness on the aerodynamically generated noise in wake-sawtooth plate interaction at a Reynolds number of 150 is numerically investigated. Two types of sawtooth plate thickness h_{thick}=0.2D and h_{thin}=0.02D are investigated. Flow simulations are carried out using direct numerical simulation and the noise calculations are solved using Curle's equation. It is found that the wake-plate interaction is more prominent for the thicker plate. Consequently, the generated aerodynamic force is bigger for thick plate than the thin plate. Sound generated from the thin plate is approximately 0.34 dB lower than the thick plate. For the sound that is due to the quadrupole source gives ± -70 dB.

Keywords: Aerodynamic sound, Bluff body, Serrations, Acoustic analogy.

Author Correspondence, e-mail: lializarose@mail.com

doi: http://dx.doi.org/10.4314/jfas.v9i7s.24

1. INTRODUCTION

Noise generation in airfoil is of concerns in many engineering applications, such as aircraft, submarine, and wind turbine. An airfoil in a turbulent flow experiences a fluctuating lift which has been proven by previous studies including Arbey & Bataille [1] and Migliore & Oerlemans [2], to radiate sound to the far-field. This fluctuating lift is a result of the unsteady pressure field produced by the airfoil in response to the turbulence. Principally, the sound generation takes place at both leading edge (LE) and trailing edge (TE) of the airfoil. The LE noise, or in some case, it is often referred to the airfoil-turbulence-interaction (ATI) noise, can be dominant if the airfoil is subject to a high intensity turbulence. Migliore & Oerlemans [2] reported up to 24 dB higher noise levels from the LE when flow with an impinging turbulence intensity of I_t =0.09. While on the other hand, the TE noise is said to be dominant when the upstream turbulence is low. The wake, tip-vortex, surface boundary layer, and transition of laminar and turbulent are among the playing factors in the TE noise generation mechanism [3].

Methods in reducing noise generation of the airfoil have been proposed by many ways. They can be classified into the source control and radiation control methods. Serrations structure applied at the LE have the ability to function in both methods. The LE serration is a bio-mimetic control method that takes the idea of the comb-like-fringe on the front margin of the owls' feathers. These serrations are supposed to be involved in the noise reduction during the owls' flight [4,5,6]. The earliest to propose this idea is Graham [7] who suspects that the main function of the LE comb is to locally reduce the velocity of the incoming flow and, additionally to deflect the flow so that it meets the leading edge under a smaller angle. The LE comb affects the boundary layer from the upstream making it to become turbulent, thus prevent the acoustically unfavorable processes [8]. Regarding the acoustic effect, as the flow is kept attached due to the serrations presence, the boundary layer thickness is affectively reduced, leading to a reduced noise generation at the TE as discussed in Lilley [3]. Also, the generation of streamwise vortices from the LE serrations reduces the coherence of the wake and several studies have shown evidence of this streamwise vortex formation [9]. Due to varying locations of separation along the spanwise direction, the separation line becomes interrupted and this lessen the coherence of vortex shedding in the wake hence leads to

suppression of tonal vortex shedding noise from the airfoil [10].

In owls' case, Weger [6] has provided improved description on how the size and shape as well as the occurrence of serrations, vary between different owl species. In summary, a serration configuration (if based on the owls' natural structure), must consist of detached barb tip, bending of the tip as well as the serration length. Most current studies [11,12] have serrations wavelength and amplitude as their parameter to investigate noise reduction. A good agreement is found as the detached barb tip can refer to the serration tooth, while serration amplitude can refer to the serration length. Until current state, the smaller the serration wavelength and the bigger the serration amplitude would result in best noise reduction [11, 13, 14], while most investigations proved the effectiveness of LE serrations, or the best LE serrations configuration in reducing airfoil noise, very few study highlights on the physics and mechanism behind how the noise can be reduced.

What is not well known is, how every single serrations' sawtooth plays its role in noise reduction and how among the saw teeth of serrations correlate and interact to perform noise reduction mechanism as a whole. Therefore, current study is an early step to discover the physics behind noise reduction promoted by the LE serrations. This study focuses on a single sawtooth and the flow physics behind the noise generation alteration. The study is held in low Reynolds number for easier understanding at this early stage of discovery.

2. NUMERICAL PROCEDURE

The aerodynamic noise calculation starts with simulating a low Reynolds number (Re=150) laminar flow using the DNS (Direct Numerical Simulation) method. Using this flow simulation, the sound source (in this case the time gradient of the lift force) is obtained. After the sound source is obtained, the sound propagation is then calculated using the Curle's equation [15].

The primitive variables of the flow fields are governed by the incompressible three-dimensional Navier Stokes euations:

$$\frac{\partial u_i}{\partial t} + u_j \frac{\partial u_i}{\partial x_j} = -\frac{1}{\rho_0}\frac{\partial p}{\partial x_i} + \frac{\partial}{\partial x_j}\left[\nu \left(\frac{\partial u_i}{\partial x_j} + \frac{\partial u_j}{\partial x_i}\right)\right] \qquad (1)$$

$$\frac{\partial u_i}{\partial x_i} = 0 \qquad (2)$$

where subscripts i and j both equal to 1,2,3. Here x_1, x_2 and x_3 denote streamwise, cross-stream and spanwise directions, respectively. U_1, U_2 and U_3 are the corresponding velocity components; u'_i depicts the fluctuating part of the velocity; ρ is the density of the fluid and p represents the fluid pressure. The open source computational fluid dynamics (CFD) code OpenFOAM is used for simulating the flow. The temporal term is discretized using second order backward scheme and the convection term is discretized using second order QUICK scheme.

The sound propagation is estimated by the equations from the Lighthill acoustic analogy [16]

$$\left(\frac{\partial^2}{\partial t^2} - c_0^2\nabla^2\right)(\rho - \rho_0) = \frac{\partial^2 T_{ij}}{\partial x_i \partial x_j}(x,t) \qquad (3)$$

$$T_{ij} = \rho u_i u_j - \tau_{ij} + \delta_{ij}((p - p_0) - c_0^2(\rho - \rho_0)) \qquad (4)$$

Eq. (3) is an inhomogenous wave equation derived from rearrangement of Navier-Stokes equations. T_{ij} is Lighthill's stress tensor, where the first term at the right hand side of Eq. (4) ($\rho u'_i u'_j$) is the Reynolds stress tensor; τ_{ij} denotes viscous stress, δ_{ij} is Kronecker delta, ρ and p are the instantaneous density and pressure, respectively. Subscript `$_0$' represents the ambient pressure.

In the current study, considering a compact body presents in the flow (i.e. the square cylinder), the free-field Green's function is used to solve the Lighthill's equations [16]. As the dimension of the body is very small compared to the wavelength i.e. ratio of wavelength to body dimension is 88.2 as according to author in previous investigation [17], the sound source are assumed compact. In the case of a compact, fixed, and rigid body, emission time variation along the body can be neglected. Hence, $r \approx |\mathbf{x}|$. Therefore, taking P_{ij} as pressure, y as the point on the rigid surface, and instantaneous force F_i of fluid on the body (i.e. lift and drag) as

$$F_i(t_r) \approx \int_S [P_{ij}]_{\tau=t_r} n_j \, dS(y) \qquad (5)$$

the Curle's solution for a fixed rigid compact body is

$$p'(x,t) = \frac{1}{4\pi c_0}\frac{\partial^2}{\partial x_i x_j}\int \frac{T_{ij}}{r}dV - \frac{1}{4\pi}\frac{\partial}{\partial x_i}\left[\frac{F_i}{r}\right]$$
$$= \frac{1}{4\pi c_0^2}\frac{x_i x_j}{x^3}\int \frac{\partial^2 T_{ij}}{\partial t^2}dV - \frac{1}{4\pi c_0}\frac{x_i}{r^2}\left[\frac{\partial F_i}{\partial t}\right] \quad (6)$$

3. COMPUTATIONAL DOMAIN

Fig. 1 shows the domain size taken in the calculation. The square cylinder upstream the sawtooth plate acts as vortex generator. Distance between the square and sawtooth plate is 4D. Top and bottom boundaries are 10D and downstream boundary is 15D away from the sawtooth plate. The upstream, top and bottom boundaries are defined as inlet boundaries where the velocity is fixed to a constant free stream value (Dirichlet BC) and zero pressure gradient (Neumann BC). The outlet boundary is 15D downstream the cylinder, where the boundary conditions are opposite that of inlet (i.e. zero velocity gradient and pressure fixed at zero).

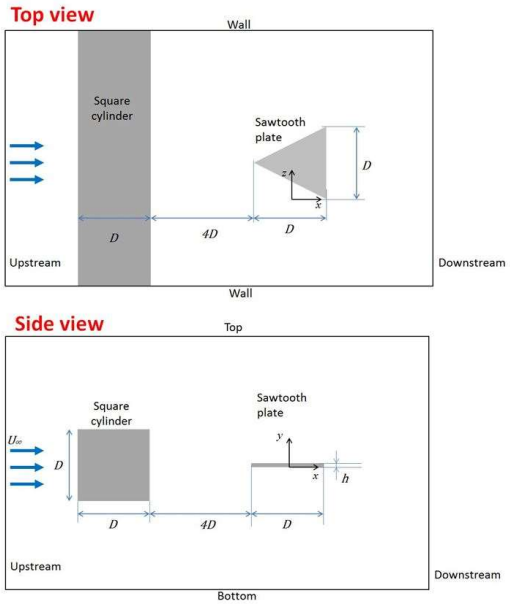

Fig.1. Sketch of computational domain

4. AERODYNAMIC RESULTS

Fig. 2 shows unsteady aerodynamic forces coefficients for both thin and thick plates. It can be noticed that the drag oscillates at approximately twice the frequency of the lift because each

vortex shed from the sawtooth plates causes the same change in drag but opposite change is in lift. This behavior is found the same as compared to the results of a circular cylinder with a splitter plate and bluff body in a tandem arrangement [18].

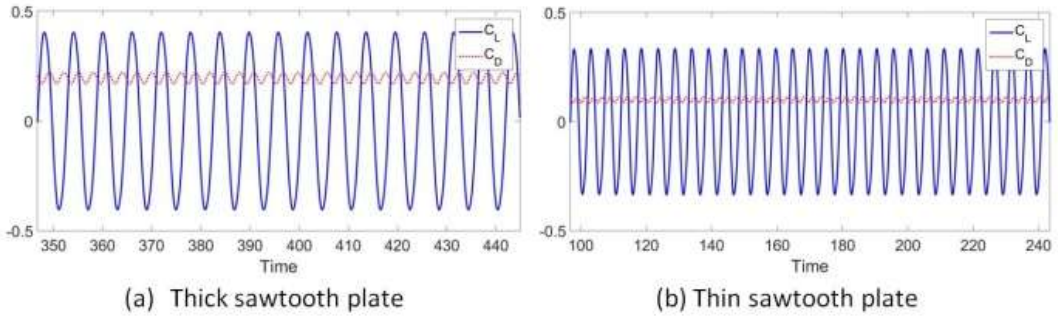

Fig.2. Fluctuations of lift and drag force coefficients acting on (a) thick and (b) thin sawtooth plate.

The root-mean-square of the lift force coefficient $C_L{}'$, mean of drag force $\overline{C_D}$ and Strouhal number St of both cases are shown in Table 1. The $C_L{}'$ and $\overline{C_D}$ of the thin sawtooth is lower than those of thick one. This can be explained based on the wake-plate interaction. As the plate becomes thinner, the velocity fluctuations around it, is reduced and consequently the surface pressure fluctuations decrease. Hence, the lift force acting on the plate is lower due to this wake-plate interaction. Magnitude of mean drag force is also lower in thin plate case. Drag force is lower due to the separated flow region is shrunk as the aspect ratio (ratio of length over the thickness) of the plate is longer. The same has been found in Prasath et al. [19]. Strouhal number $St = fD/U_\infty$ is a non-dimensional representation of the vortex shedding frequency f, while D and U_∞ depict streamwise length of the plate and the velocity of free stream, respectively. Comparing the values of St for both cases, the thin plate has higher frequency of vortex shedding.

Table 1. Global parameters

Case	Plate thickness, h	$C_L{}'$	$\overline{C_D}$	St
Thick	0.2D	0.294	0.196	0.171
Thin	0.02D	0.244	0.100	0.195

Fig. 3 shows the power spectrum density (PSD) of the forces (lift and drag) fluctuations. x-axis is showing the vortex shedding frequency and the y-axis is showing the power amplitude of lift signals from the square cylinder. In both cases, a series of peak that is harmonic with the vortex shedding frequency $(f_v, 3f_v, 5f_v \ldots nf_v)$ is observed. These appearances can be attributed to the linear interaction between the von Karman vortex of the square cylinder with the sawtooth plate in the wake [20].

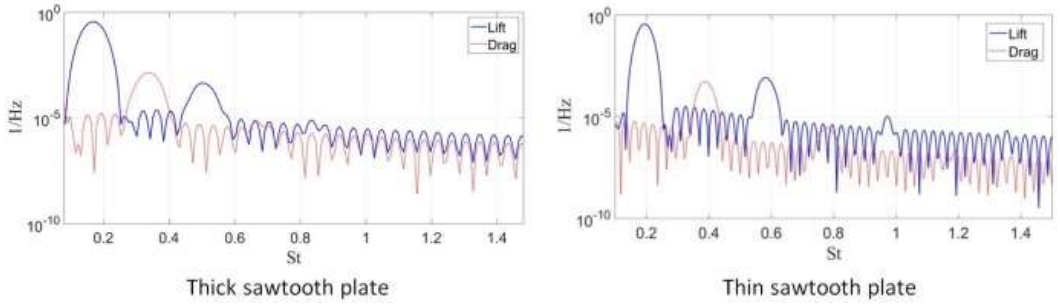

Fig.3. PSD of lift and drag force fluctuations of (a) thick sawtooth and (b) thin sawtooth plate

Fig. 4 shows contours of instantaneous vorticity magnitude at identical time when the lift is at maximum as well as the streamline showing averaged velocity in both cases. As mentioned previously, the square cylinder placed 4D upstream the sawtooth acts as the vortex generator. From Fig. 4(a) and 4(b), the vortex shedding generated from the square interferes with the presence of the sawtooth plate, thus the formation of a coherent vortex from the shear layers of square is prevented. Consequently, the vortices then undergo a process of stretching caused by the viscous effect on the surface of the sawtooth plate. After impingement on leading edge of the plate, the vortex remains attached on the leading edge and it is simultaneously stretched by the accelerating flow about the sawtooth plate. This stretching process splits the vortex that allows a weaker vortex system to form downstream of the plate. This type of vortices is named the transverse vortices according to their shedding direction.

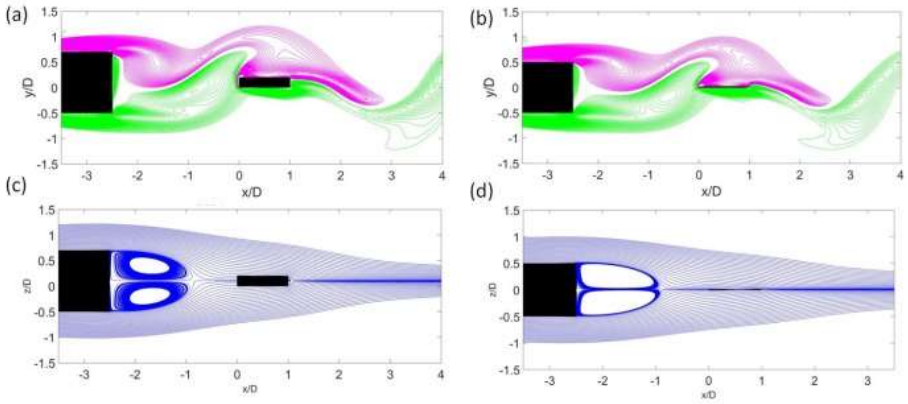

Fig.4. Vorticity contour $-3 \leq \omega D/U_\infty \leq 3$ and streamline at middle cross section of sawtooth plate (a) and (c) thick sawtooth. (b) and (d) thin sawtooth plate.

Fig.4 (c) and 4(d) show the streamline of averaged velocity. A recirculation region is formed in the wake of the square cylinder. As we can observe the saddle point is in the gap between the plate and square cylinder. The shear layers shed from both sides of square cylinder has reattached on the downstream of square cylinder.

On the other hand, the sawtooth plate can be studied in analogy to delta wing, whose it can be said to induce the counter rotating vorticity. Fig. 5(a) shows the counter-rotating vortices in delta wing flow from Chen et al. [21]. This type of vortices is attributed as the noise reduction mechanism in Chen et al. [21]. However, as in present studies, no counter-rotating-vortices are observed in the flow. Fig. 4(b) shows types of vortices present in current study.

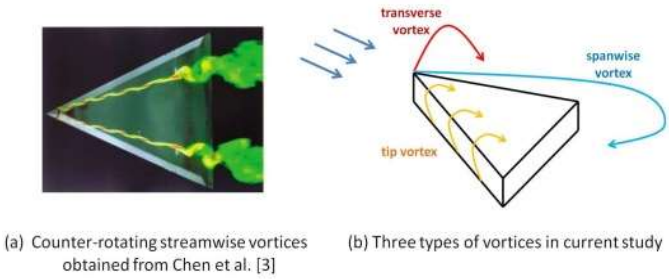

Fig.5. Types of vortices.

The pressure contour showed in Fig. 6 can be related with the forces magnitude experienced by the sawtooth plate. High pressure region on the thick sawtooth plate case is bigger than

that of the thin plat case. This exactly explains the higher lift and drag forces acting on the thick sawtooth plate. Furthermore, the dipole noise generated from the flow can also be related with this pressure contour.

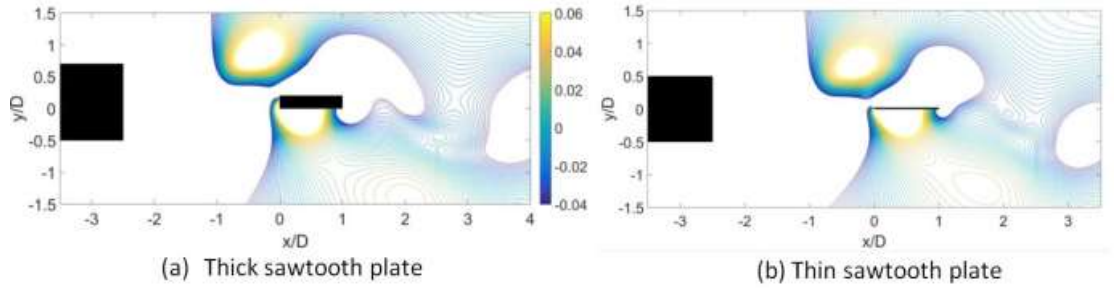

Fig.6. Pressure contour at middle cross section of sawtooth plate.

5. AEROACOUSTIC RESULTS

Aeroacoustic noise calculation is done using the Curle's theory. They can be classified according to their directivity nature and source of noise, i.e. the Dipole noise from the force fluctuations and the Quadrupole noise from the Reynolds stress.

Using Eq. (6) from Curle's Theory of Acoustics, the dipole sound directivities are calculated. Fig. 7 shows sound contour for both combined sound generated due to lift and drag forces. Sound waves radiates more in the direction of ±

This is agreed with directivity results, i.e. sound due to lift is dominated the dipole sound radiation. As it goes further from the sound source, sound pressure contour level decreases.

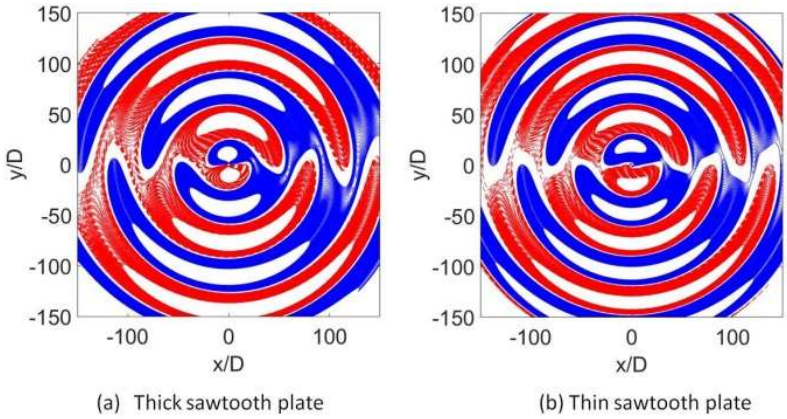

Fig.7. Dipole sound pressure contour due to both lift and drag forces.

The PSD of sound from the fluctuating forces is shown in Fig. 8. From the figure, it is

observed that the dominant contribution to the radiated tone is a source that is coherent with the force applied on the sawtooth plate. The sound is harmonic. Combined sound from the lift and drag forces is represented in black dotted line. The dipole sound is dominated by the fluctuating lift in the directivity. According to the magnitude of the dipole, the sound from thick plate has not much difference than from the thin plate.

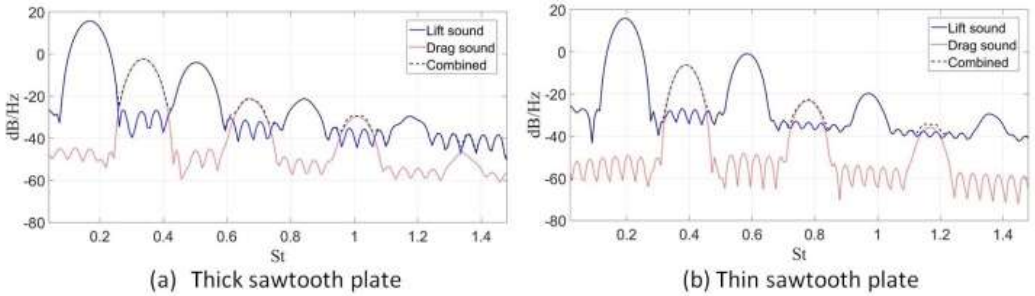

Fig.8. PSD of sound due to Lift, Drag and the combination. Blue lines: Lift sound. Red dotted lines: Drag sound. Black dotted lines: Combined sound.

Aerodynamic sound generated from flow is also emitted as a quadrupole in form. This study calculates the quadrupole noise using the second term of Eq. (6). From the equation, we can understand that the sound that is transmitted quadrupolar in form is sourced from the Reynolds stress $\rho u'_i u'_j$. The $\rho u'_i u'_j$ is a major component in the Lighthill stress tensor T_{ij}.

Fig. 9 shows the fluctuations of quadrupole sound at middle plane. Again, thin plate generated quadrupole sound approximately 11.43 dB lower than that of thick plate. However, the magnitude of the quadrupole sound is not that dominating if compared with that of dipole sound. Quadrupole sound is $\mathcal{O}\ (10^{-8})$ while dipole sound is $\mathcal{O}(10^{-3})$. Thick plate is -65.15 dB and thin plate is -76.59 dB. Decibels are a unit of a logarithmic scale. In current study case, reference sound pressure is 2×10^{-5} [Pa]. Thus the negative decibel values of quadrupole sound shows that it is lower relative to the reference sound pressure value.

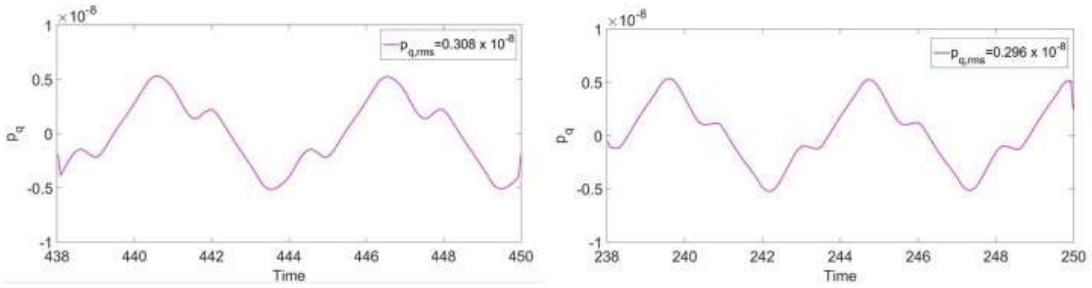

Fig.9. Fluctuations of quadrupole sound due to turbulent structures of the flow form (a) thick and (b) thin sawtooth plate.

Fig. 10 shows the Reynolds stress contour i.e. the major source of quadrupole noise generation. Reynolds stress is observed a little stronger in its intensity in the thick sawtooth plate case. Thus, this proves that the higher quadrupole noise magnitude is for the thicker plate.

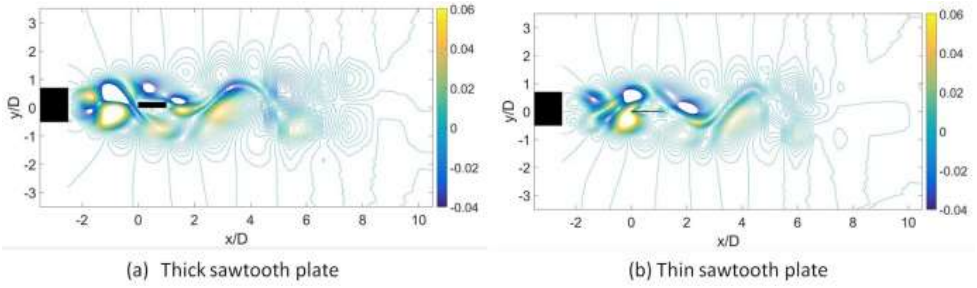

Fig.10. Reynolds stress contour at middle cross section at (a) thick and (b) thin sawtooth plate.

6. CONCLUSIONS

The flow and sound behavior of a single sawtooth plate has been numerically investigated using direct numerical simulation for the sound sources and acouctis analogy for the sound propagation. Two thicknesses (0.02D and 0.2D) of the plate are used. Flow results show the presence of three types of vortices for both thicknesses - (1) Transverse vortices (2) Spanwise vortices (3) Tip vortices. However, the aerodynamic forces acting on the thicker plate is bigger than the thinner plate. This is due to the stronger wake-plate interaction for the thicker plate than the thinner plate. Thick plate it 0.34 dB louder than the thin plate. For both plate thicknesses, the radiated sound is dominated by the fluctuating force (dipole sound source)

where the sound due to the quadrupole sound source is 10^3 order of magnitude smaller than the dipole sound source.

7. REFERENCES

[1] Arbey, H and Bataille, J., (1983) Noise generated by airfoil profiles placed in a uniform laminar flow, Journal of Fluid Mechanics 134 33-47.

[2] Migliore, P and Oerlemans, S., (2003) Wind Tunnel Aeroacoustic Tests of Six Airfoils for Use on Small Wind Turbines, National Renewable Energy Laboratory, Golden, Colorado, December 80401-3393

[3] Lilley, GM., (1998) A study of the silent flight of the owl, 4th AIAA/CEAS Aeroacuostics Conference, Toulouse, France, 1998-2340

[4] Bachmann, T. and Wagner, H., (2011) The three-dimensional shape of serrations at barn owl wings: towards a typical natural serration as a role model for biomimetic applications, Journal of Anatomy 219 (2) 192-202. doi:10.1111/j.1469-7580.2011.01384.x

[5] Bachmann, T., Klan. S., Baumgartner, W., Klaas, M., Schroder, W. and Wagner, H., (2007) Morphometric characterization of wing feathers of the barn owl Tyto alba pratincola and pigeon Columbia livia, Front Zool 4 1-15.

[6] Weger, M and Wagner, H, (2016) Morphological Variations of LEading Edge Serrations in Owls (Strigiformes) PLoS ONE 11(3)

[7] Graham, RR, (1934) The silent flight of owls, Journal of Royal Aerospace Society 38 837-843.

[8] Hertel, H., (1963) Struktur, Form, Bewegung. Otto Krauskopf-verlag Mains [translated version: Milton S. Katz, Structure, Form, Movement. Reinhold, New York (1966)

[9] Hansen, K., Kelso, RM. and Doolan, CJ., (2010) Reduction of flow-induced tonal noise through Leading edge tubercle modifications, 18th AIAA Aeroacoustic Conference.

[10] Hansen, K., Doolan, CJ. and Kelso, RM., (2012) Reduction of flow-induced airfoil tonal noise using Leading edge sinusoidal modifications, Acoustics Australia

[11] Haeri, S., Narayanan, S. and Joseph, P., (2014) 3D Calculations of aerofoil-turbulence interaction noise and the effect of wavy leading edges, AIAA/CEAS Aeroacoustic Conference June, 1-15

[12] Kim, JW., Haeri, S. and Joseph, P., (2016) On the Reduction of Aerofoil-Turbulennnnnce Interaction Noise Associated with Wavy Leading Edges, Journal of Fluid Mechanics (792)526-552

[13] Kim, JW. Haeri, S and Jospeh, P., (2015) In the Mechanisms of Noise Reduction in Aerofoil-turulence interaction by using wavy leading edges, AIAA/CEAS Aeroacoustic Cenference 1-18

[14] Narayanan, S., Joseph, P., Haeri, S., Kim, JW., Chaitanya, P. and Polacsek, C., (2014) Noise Reduction Studies from the Leading Edge of Serrated Flat Plates, AIAA/CEAS Aeroacoustics Conference June Atlanta, GA, 1-14

[15] Curle, N., (1955) The influence of solid boundaries upon aerodynamic sound, Proceedings of the Royal Society London. Series A, Mathematical and Physical Sciences, 231 (1187) 505-514.

[16] Lighthill, ML., (1952) On sound generated aerodynamically 1: General Theory, Proceedings of the Royal Society London. Series A, Mathematical and Physical Sciences, 211 (1107) 564-514

[17] Samion, SRL., Ali, MSM., Abu, A., Doolan, CJ., and Porteous, RCY., (2016) Aerodynamic sound from a square cylinder with a downstream wedge, Aerospace Science and Technology 53 85-94.

[18] Doolan, CJ., and Leclercq, DJJ., (2009) The interaction of a bluff body with a vortex wake, Journal of Fluid Structures 25 (5) 867-888.

[19] Prasath, SG., Sudharsan, M., Kumar, VV., Diwakar, SV., Sundarajan, T., and Tiwari, S., (2014) Effect of aspect ratio and orientation on the wake characteristics of low Reynolds number flow over a triangular prism, Journal of Fluid Structures 46 59-76.

[20] Hansen, K., Doolan, CJ. and Kelso, RM., (2012) Reduction of flow-induced airfoil tonal noise using Leading edge sinusoidal modifications, Acoustics Australia

[21] Chen, W.J., Qiao, WY., Tong, F., Duan, WH., Liu, TJ., Wang, XN. and Liu, XQ., (2016) An Experimental and Numerical Investigation of Airfoil Instability Noise with Leading Edge Serrations, AIAA/CEAS Aeroacoustic Conference, 30 May - 1 June Lyon, France

How to cite this article:
Samion S R L, Ali M S M, and Doolan C. Aerodynamic sound from a sawtooth plate with different thickness. J. Fundam. Appl. Sci., 2017, *9(7S), 241-254.*